Mon. Not. R. Astron. Soc. **276,** 1255–1261 (1995)

Estimating distances to elliptical galaxies with a mass–luminosity relation

T. S. van Albada,[1,2] G. Bertin[2] and M. Stiavelli[2]
[1] *Kapteyn Instituut, Rijksuniversiteit Groningen, Postbus 800, 9700 AV, Groningen, The Netherlands*
[2] *Scuola Normale Superiore, Piazza dei Cavalieri 7, I 56126, Pisa, Italy*

Accepted 1995 May 12. Received 1995 May 5; in original form 1994 August 2

ABSTRACT

We argue that the physical reason for the success of the Fundamental Plane and the D_n–σ relation as distance estimators for elliptical galaxies is the existence of a relation between luminosity and mass with small intrinsic scatter. Therefore a better understanding of the luminosity and mass variables, and of the mass–luminosity relation, is needed to improve distance estimation for elliptical galaxies. We propose a distance indicator in the form of a mass–luminosity relation and use it to derive modifications to the Fundamental Plane and to the D_n–σ relation. Note that distances estimated with these modified Fundamental Plane and D_n–σ relations may, in practice, turn out to be less precise than those estimated with the standard relations when the added terms have large observational errors.

Key words: galaxies: distances and redshifts – galaxies: elliptical and lenticular, cD – galaxies: fundamental parameters – galaxies: photometry – distance scale.

1 INTRODUCTION

Luminosities of ellipticals can be accurately predicted by means of two distance-independent quantities: the central velocity dispersion σ_0 and the mean surface brightness SB_e inside the effective radius R_e (Djorgovski & Davis 1987; Dressler et al. 1987). Put differently, ellipticals are confined to a surface in the L, σ_0, SB_e space, with remarkably small scatter in the perpendicular direction. This is the so-called Fundamental Plane (FP).

An important ingredient determining the existence and thickness of the FP is the mass–luminosity relation for ellipticals (Faber et al. 1987), with mass being measured by $\sigma_0^2 R_e/G$. The other ingredients determining the nature of the FP are the similarity of the radial structure of ellipticals (homology) and the fact that they are in equilibrium, which allows the use of the virial theorem. Thus the thickness of the FP is determined mainly by the spread in the mass–luminosity relation and by the degree of homology; see Faber et al. (1987), Bender, Burstein & Faber (1992, hereafter BBF) and Section 2.

In this paper, we focus on the connection between the FP and the mass–luminosity (M–L) relation for ellipticals. Our starting point is that the main reason why the FP, and its close relative, the D_n–σ relation, can be used as distance estimators is the existence of a M–L relation for ellipticals with small intrinsic scatter. This is so because only the M–L relation contains information that can be used as a distance indicator ($M \propto$ *distance*; $L \propto$ *distance*^{2}). The other two factors determining the FP (similar radial structure and equilibrium) contain no information relevant for distance estimation. Thus, in order to improve distance estimation for ellipticals, one should first accurately determine the M–L relation and try to understand the sources of scatter in it. In fact, one may argue that there is no need to use the FP or the D_n–σ relation for distance estimation: if feasible from the observational point of view, one might as well use the underlying M–L relation directly (see Section 4, equation 5). In this approach, homology is no longer a requirement *per se*: deviations from homology can, in principle, be incorporated in the determination of M and L. In any case, the M–L approach facilitates the calibration of the D_n–σ relation with galaxies in the Local Group (Dressler 1987), because it provides a useful framework for the extension of the D_n–σ relation to S0 galaxies and bulges of spirals (see the discussion by Saglia, Bender & Dressler 1993, hereafter SBD).

Several studies have found that the scatter about the FP can be reduced by replacing the velocity dispersion σ by a combination of σ and a rotation term V/σ, and by adding a metallicity term (e.g. Guzmán et al. 1992; Djorgovski & Santiago 1993; Jørgensen, Franx & Kjærgaard 1993, hereafter JFK; SBD). In the following, we show how these results can be clarified in the framework of a mass–luminosity relation as the basis of the FP.

Our discussion will concentrate on the following issues.

(i) What is the best way to measure 'mass', and to what extent is the scatter about the FP caused by the use of an 'incomplete' mass estimator like $\sigma_0^2 R_e/G$?

(ii) What is the most suitable luminosity variable? Ellipticals show a range in the Mg_2 index, and therefore in metallicity and/or age. Presumably, then, luminosities should be corrected for differences in the underlying stellar populations.

(iii) What is the precise relation between luminosity and mass? The M–L relation underlying the FP is $L \propto M^{\alpha}$, but perhaps a power law is too naïve, and a more accurate estimator would require the use of a non-power-law relation.

The discussion is complicated by the likely presence of dark haloes, which causes problems with the definition of mass M. For most of the following discussion an 'operational' definition of mass through $\sigma^2 R/G$ (i.e., not based on any assumption regarding dynamical state or the presence of dark matter) is adequate, but, in some instances, we assume explicitly that the distribution of matter follows that of light.

2 THE ORIGIN OF THE FUNDAMENTAL PLANE AND THE D_n–σ RELATION

The following argument illustrates how the origin of the FP can be traced to the existence of a well-defined mass–luminosity relation for ellipticals, which is just what we need for a distance indicator. Let us postulate as a 'standard candle' for ellipticals: $L=f(M) \propto M^{\alpha}$, where M is the mass as measured by $\sigma_0^2 R_e/G$. Next, write $L \propto I_e R_e^2$ and put $\alpha = 0.807$. Then one recovers the equation for the FP:

$$R_e \propto \sigma_0^{1.35} I_e^{-0.84}, \tag{1}$$

as given by Faber et al. (1987); see also BBF. The D_n–σ relation is a close approximation to the FP (Section 5). Therefore, the success of that relation as a distance estimator also relies on the close coupling of the mass and luminosity of ellipticals. It should be stressed that the above derivation of the FP assumes that ellipticals are 'homologous' at fixed L and M, i.e., that the proportionality constants in the expressions for L and M do not vary among ellipticals of similar luminosity and mass. When this condition is not met, or when the relation between M and L is not one-to-one, this will result in a thickening of the FP. (Note that we do not require homology for different values of L and M, since such non-homology would just be reflected in a change in the shape of the M–L relation).

In the literature, expressions may be found for the FP which cannot be reduced to the form $L \propto M^{\alpha}$, or equivalently to $I_e R_e^2 \propto (\sigma_0^2 R_e)^{\alpha}$. Then a 'second parameter' would be required, e.g., $L \propto M^{\alpha} R_e^{\beta}$. However, given the uncertainties in the coefficients for the FP, we have not found convincing evidence for the need for a second parameter.

3 MEASURING MASSES AND LUMINOSITIES

Before the standard candle law $L=f(M)$ can be introduced, the mass M of the galaxy and its luminosity L must be defined. Ellipticals are probably surrounded by dark haloes, and the stellar population may vary with radius. It is not obvious, therefore, what mass one should attempt to measure and what luminosity one should use. Below, we discuss these issues in some detail.

3.1 Masses

The mass used in the description of the FP,

$$M = \beta \sigma_0^2 R_e/G, \tag{2}$$

is simply the quantity obtained by dimensional analysis from a given 'central' velocity dispersion σ_0 and effective radius R_e. Note that for $\beta \approx 4.9$ this is the total mass of a galaxy for which light traces mass, characterized by an $R^{1/4}$-law profile (all the way in to the centre), and by an isotropic velocity distribution (Michard 1980; Bailey & MacDonald 1981). The main issue discussed below is whether an alternative mass estimator might lead to a smaller scatter in the mass–luminosity relation, and hence to a smaller scatter about the FP. If so, this would be beneficial for distance estimation.

We first note that the likely cause of the well-defined mass–luminosity relation for ellipticals is the uniformity of the (old) stellar population in these systems, suggesting that the basic standard candle is $L=f(M_*) \propto M_*^{\alpha}$, where M_* is the total *stellar* mass. The quantity of interest would then be the *stellar* mass-to-light ratio. At first sight this quantity can best be measured at the centre, because the likely presence of dark haloes will affect measurements made at larger radii. However, given the large variation in core properties and the fact that these are very difficult to measure reliably, we reject this approach. Clearly, a more *global* measurement of mass and luminosity is called for. However, in doing so one must face several complications: dark haloes, rotation, and departures from spherical symmetry. These can only be dealt with by constructing models of individual galaxies, based on the extended mean rotation and velocity dispersion profiles now becoming available for many galaxies (see, e.g., Binney, Davies & Illingworth 1990, hereafter BDI; Carollo 1993; ven der Marel & Franx 1993; Bertin et al. 1994). However, such a task is not easy, due to our limited knowledge of the intrinsic shape and dynamical state of ellipticals.

As a compromise in this direction, consider the possibility of modifying equation (2). Potential shortcomings of that equation are (i) it assumes that ellipticals are homologous, and (ii) σ_0 is sensitive to the detailed structure of the core. A discussion of the former objection, i.e., the homology issue, falls outside the scope of this paper. The latter objection can, in principle, be remedied by using a velocity dispersion averaged over a larger area (see below), but at the cost of the complications mentioned above. This strategy has been considered by JFK, who propose to replace σ_0^2 in the FP by the luminosity-weighted second moment of the velocity profile $\langle v^2 \rangle$, which includes rotation if present, inside a radius of order $0.5 R_e$. When averaged over the *entire* galaxy, $\langle v^2 \rangle$ does indeed have the advantage that its value does not depend on the orbital structure of the system, e.g., pressure or rotation support; see Appendix A. It remains to be seen whether this property is still present when the average is restricted to smaller apertures.

To see how some of the factors that are ignored when using equation (2) translate into effects on distance estimates, we have calculated a number of equilibrium models to explore how the quantity $\sigma^2 R_e$ varies with viewing angle and with 'dynamical state', in particular, with the amount of rotation present, for galaxy models of the same mass. Previous work based on the tensor virial theorem (e.g. JFK; SBD) shows that ellipticals, when seen from different directions, project mainly *along* the FP, i.e.

$$R_e \sigma_0^{-1.35} I_e^{0.84} \simeq \text{constant}, \qquad (3)$$

for a given elliptical galaxy seen from different viewing directions. This condition can be rewritten by noting that the luminosity remains constant (on the assumption that internal obscuration is unimportant); therefore $I_e R_e^2 = \text{constant}$. Inserting this in equation (3), one finds that $\sigma_0^2 R_e \simeq \text{constant}$. In other words, projection *along* the FP is equivalent to the statement that variations in σ_0^2 and in R_e tend to balance each other when an elliptical is seen from different directions.

Our models are oblate systems with a range in rotation speeds and a density distribution following a modified Jaffe law; details are given in Appendix A. In a broad sense they confirm the earlier results. We find that for our models the value of $\langle v^2 \rangle_{0.5 R_e} R_e$ is remarkably constant when the viewing direction is varied; the subscript indicates an average over an aperture with radius $0.5 R_e$. This is shown in Fig. 1, where we plot $\langle v^2 \rangle_{0.5 R_e}$ versus R_e. The prediction by the virial theorem (VT), on the other hand, deviates considerably from the curve $\langle v^2 \rangle R_e = \text{constant}$. Note that the models approach the VT prediction when the aperture is increased; see Appendix A. By adding a massive, extended dark halo (either spherical or flattened) to our Jeans models, we have verified that the derived dependence of $\langle v^2 \rangle_{0.5 Re} R_e$ on viewing angle is maintained.

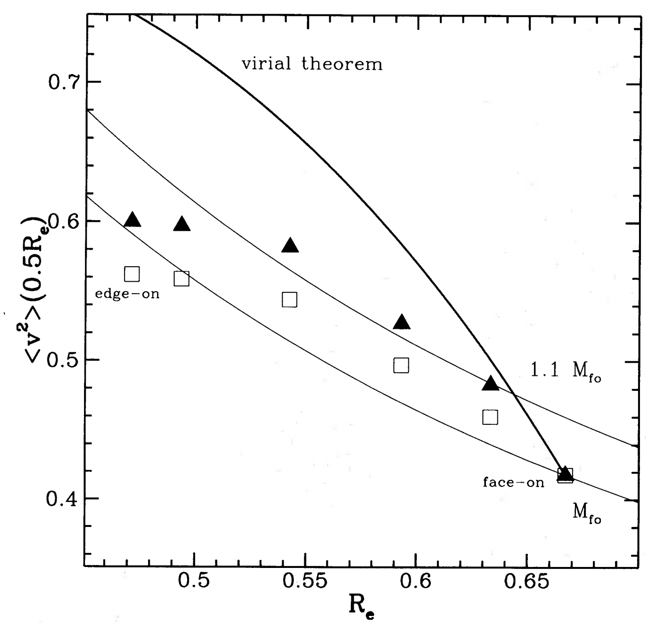

Figure 1. Behaviour of $\langle v^2 \rangle R_e$ for an E5 oblate galaxy model when the viewing direction is altered. Motion *along* the Fundamental Plane does not affect the estimated distance; this requires $\langle v^2 \rangle R_e = \text{constant}$. $\langle v^2 \rangle_{0.5 R_e}$ represents the second moment of the velocity profile, averaged over a circular aperture with radius $0.5 R_e$ (luminosity-weighted); by definition, it includes rotational motion when present. R_e has been obtained by fitting an $R^{1/4}$ law to the luminosity profile; for details, see Appendix A. Open squares: non-rotating models. Solid triangles; Isotropic rotators. Thick solid line: virial theorem, using the equations given in Appendix A, scaled to our face-on model. Thin lines: curves of constant $\langle v^2 \rangle R_e$ (corresponding to $M_{\text{face-on}}$ and $1.1 M_{\text{face-on}}$). Note that for our models the value of $\langle v^2 \rangle R_e$ is conserved much better when the viewing angle is varied than anticipated from the application of the virial theorem.

In conclusion, the virial mass estimator $M = \beta \langle v^2 \rangle R_e / G$, where β is a constant and $\langle v^2 \rangle$ represents an average over the entire galaxy, has the nice property that M does not depend on the orbital structure of the system. A drawback, however, is that, for a given mass, $\langle v^2 \rangle R_e$ depends considerably on viewing angle for flattened systems (see equation A11 and Fig. 1), and for that reason it is not to be recommended as a mass estimator. We find that by using circular apertures of small size, with radius $0.5 R_e$, the 'mass' estimated by $\langle v^2 \rangle_{0.5 R_e} R_e$ is only weakly dependent on viewing angle, but at the cost of introducing a small dependence on the detailed dynamical structure of the system.

3.2 Luminosities

Elliptical galaxies show a large range in 'metallicity', as measured for instance by the Mg_2 index, and their stellar populations will therefore differ (see, e.g., Burstein et al. 1988; de Carvalho & Djorgovski 1992; Guzmán et al. 1992). Such variations in the stellar populations among ellipticals will lead to variations in luminosity at fixed (stellar) mass M_*, and this may be a source of error for distance determinations. Therefore it would be best to use population-corrected luminosities (see, e.g., Guzmán & Lucey 1993), but, as will be discussed below, it is not clear whether this is feasible in practice.

Attempts to find a possible dependence of the FP on metallicity give contradicting results. Lynden-Bell et al. (1988) and Burstein, Faber & Dressler (1990) find no evidence for an Mg_2 dependence in the sample of cluster and field galaxies of Faber et al. (1989) (see, however, Appendix B). On the other hand, Guzmán & Lucey (1993) do find an Mg_2 effect in Coma.

Population synthesis studies show that the effects of age and metallicity on the integrated mass-luminosity ratio are difficult to separate (Worthey 1994), even with carefully selected indices. For our discussion the cause of a spread in L/M_* (i.e. age, Z or IMF) does not really matter. The important point is that, when the variation in L/M_* is linked to a spread in the strength of the Mg_2 feature, in principle, it is possible to define a population-corrected luminosity empirically, e.g.,

$$\log L_{pc} = \log L_{obs} + \text{constant} \times \delta Mg_2. \qquad (4)$$

Results of population synthesis models give some support for such an approach. For single-burst models, for example, Worthey (1994) finds, in the neighbourhood of age $= 12 \times 10^9$ yr and [Fe/H] $= -0.5$, that M_*/L_B increases with increasing Mg_2 index, for constant-age sequences as well as for constant-[Fe/H] sequences. The coefficients are, however, very different for these two cases: $\delta \log(M_*/L_B)/\delta Mg_2 \simeq 1.8$ for a constant-age sequence, and 12 for a constant-[Fe/H] sequence. In view of the marginal observational evidence for a metallicity term in the FP, and the uncertainty in the theoretical coefficient, a proposal to apply a correction of this type seems premature.

4 THE MASS-LUMINOSITY RELATION FOR ELLIPTICAL GALAXIES

Let us now proceed to investigate the shape of the M–L relation for ellipticals. In particular, we want to investigate whether the power law $L \propto M^{\alpha}$ underlying the equation for the FP (see Section 2) is adequate. For such an analysis one should, ideally, use masses obtained from a detailed mass-modelling procedure and luminosities that have been corrected for variations in the stellar content among ellipticals. However, such data are not yet generally available. Furthermore, one should use distances that conform to a fairly sophisticated model of the flow of galaxies in the nearby Universe. Velocity-field models, however, are themselves based on distance estimators like the D_n–σ relation. Therefore a proper analysis of the M–L relation is a complex undertaking that requires an *iterative* procedure.

In the discussion below we use data for the ellipticals in the so-called 7S sample (Faber et al. 1989). We consider three assumptions for deriving distances to individual ellipticals. (i) *Galactocentric* distances. These are based on a smooth Hubble flow with $H_0 = 50$ km s^{-1} Mpc^{-1}, using heliocentric velocities listed by Faber et al. and corrected to the Galactic standard of rest following RC3 (de Vaucouleurs et al. 1991). (ii) *Virgocentric* distances. These have been calculated following Kraan-Korteweg (1986), using the middle distance for cases with triple solutions. (iii) *CMB* distances. For these the recession velocities in the CMB rest frame, as given by Faber et al., have been used. To avoid circular reasoning we do not consider a Great Attractor flow model. Masses have been calculated using equation (2) with $\beta = 5$, and we use total B luminosities corrected for various effects as given by Faber et al. (1989). No correction for Malmquist bias has been applied.

The resulting mass–luminosity relations are shown in Fig. 2 (upper panels) for ellipticals from Faber et al. (1989) with data-quality parameters 1 and 2. The straight lines are 'impartial' least-squares fits. The plots show that the relation between $\log L$ and $\log M$ is not strictly linear. There is evidence for changes in slope near $\log M \approx 11$, 11.5 and 12. The wiggles are shown more clearly in the lower panels of Fig. 2, where we plot the deviations $\delta \log L$ from the power laws drawn in the upper panels.

Clearly, the shape, as well as the scatter, of the M–L relation that we derive is affected not only by the flow model adopted, but also by the choice of the sample and by the estimators of M and L. Yet similar smaller scale features are present for all three flow models, indicating that deviations of the M–L relation from a simple power law may be important.

We have also applied a Kolmogorov–Smirnov test to the distributions of $\log M$ values of the points above and below the lines in Fig. 2, and find them to be different at the 99.9 per cent level or higher for all three distance models.

The underlying cause for a mass–luminosity relation as given in Fig. 2 is not clear. A combination of several factors may be responsible. Note that masses have been calculated with equation (2), and thus are subject to the comments and cautionary remarks given earlier (Section 3). Indeed, the masses represent an unknown mixture of luminous and dark matter that may well vary in a systematic way along the sequence of elliptical galaxies (see also BBF and Guzmán, Lucey & Bower 1993). Note also that the shape of the initial mass function above and below the main-sequence turn-off, affecting the amount of matter locked up in stellar remnants and low-mass stars, might correlate with the mass of the system (cf. Renzini & Ciotti 1993). In any case, there is no reason to expect a 'simple' mathematical relation between M and L. We stress that these unresolved questions do not hamper the use of the M–L relation for distance estimation.

The mass–luminosity relation $L = q(M) M^{\alpha}$ can be used as a distance estimator by interpreting it as the locus in M–L space upon which all ellipticals must lie. Application of this relation in practice proceeds as follows. Let ($M_{\rm H}$, $L_{\rm H}$) be mass and luminosity using the Hubble distance $D_{\rm H}$, and let the true distance be D. Then $M = (D/D_{\rm H}) M_{\rm H}$ and $L = (D/D_{\rm H})^2 L_{\rm H}$. Inserting these expressions for M and L in the M–L

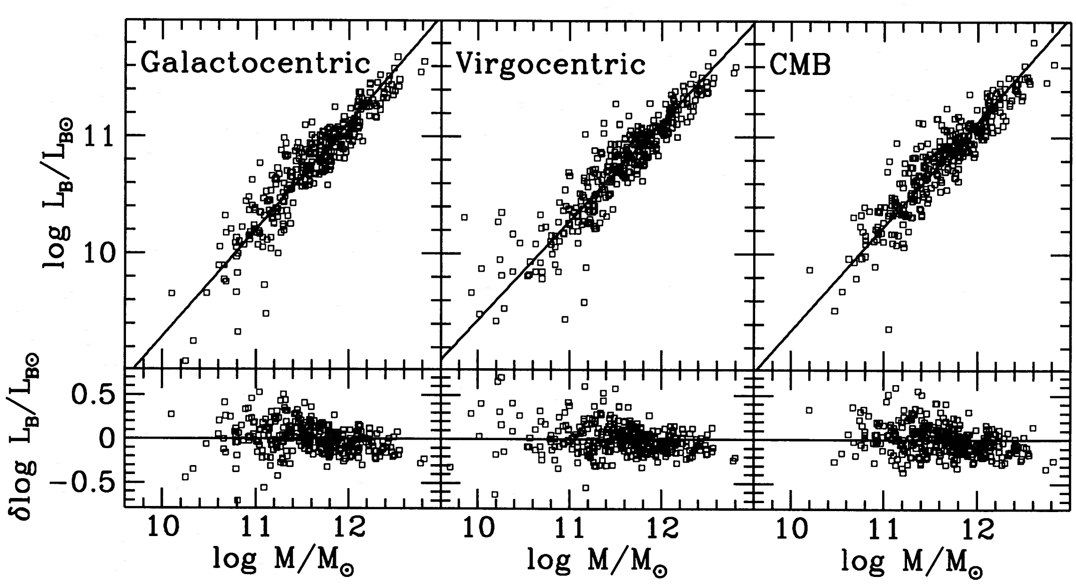

Figure 2. Upper panels: mass–luminosity relations for a sample of 321 elliptical galaxies from Faber et al. (1989), using three flow models, indicated in the panels; see text. In the lower panels residuals with respect to the power laws drawn in the upper panels are plotted.

relation and solving the resulting expression for $D/D_{\rm H}$, one finds, with $\alpha = 0.82$,

$$\log(D/D_{\rm H}) = 0.85 \log q(M_{\rm H}) + 0.69 \log(M_{\rm H}/L_{\rm H}) - 0.16 \log L_{\rm H}, \quad (5)$$

where we have approximated the factor $q(M)$ by $q(M_{\rm H})$. This expression shows that the main sources of uncertainty in the distance are the intrinsic dispersion and the observational error in the mass-to-light ratio. In Section 3.1, we found a dispersion in M for oblate models, with different amounts of rotation and seen from different directions, of order 5 per cent due to the use of an approximate mass estimator. Equation (5) shows that 70 per cent of this dispersion will be found back in the derived distances. Fig. 2 shows that the variation in the factor $\log q(M_{\rm H})$ is about 0.1 dex. Neglect of the difference between the 'true' mass–luminosity relation and a power law can therefore lead to large systematic effects, up to 20 per cent in the distances for certain mass intervals.

5 GENERALIZED FUNDAMENTAL PLANE AND D_n–σ RELATION

The results obtained so far can be summarized by saying that the standard-candle law underlying the Fundamental Plane and D_n–σ relation is a mass–luminosity relation of the form $L_{\rm pc} = q(M) M^{\alpha}$. The factor $q(M)$ takes the deviation of the M–L relation from a power law into account. Preferably, M should be obtained through detailed mass-modelling; the luminosity should be corrected for variations in the stellar content. The mass–luminosity distance estimator can be transformed into a 'generalized' FP by rewriting the mass and luminosity variables. Using, for example, equation (2) for M, $\log L_{\rm pc} = \log L_B + 1.8\,\delta Mg_2$ (constant age), $\log L_B =$ constant $- 0.4 SB_{\rm e} + 2 \log R_{\rm e}$, and $\alpha = 0.82$, one finds:

$$\log R_{\rm e} = \text{constant} + 0.69 \log\langle v^2\rangle + 0.34 SB_{\rm e} + 0.69 \log \beta - 1.5\,\delta Mg_2 + 1.85 \log q(M). \quad (6)$$

Compared to the traditional expression for the FP, equation (6) has three additional terms, involving β, δMg_2, and $q(M)$. These terms describe, respectively, a correction factor to the mass estimator that takes deviations from homology and variations in dynamical state and viewing angle into account (see Section 3.1), a correction to the luminosity for differences in the stellar populations of ellipticals based on the Mg_2 index (assuming constant age and varying Z), and the deviation of the true M–L relation from a power law. Furthermore, σ_0^2 has been replaced by $\langle v^2\rangle$, i.e., by the second moment of the velocity profile averaged over a large aperture (see JFK). Note that $\langle v^2\rangle$ includes rotational motion when present. An extension of the FP with only an Mg_2 term (with a different coefficient than above) has been given by Guzmán & Lucey (1993).

In the same way, a generalized D_n–σ relation can be derived. Using the relation between D_n and $R_{\rm e}$ given by van Albada, Bertin & Stiavelli (1993),

$$\log D_n \simeq \log(2R_{\rm e}) - 0.289\,\Delta SB - 0.019(\Delta SB)^2, \quad (7)$$

one finds:

$$\log D_n = \text{constant} + 0.69 \log\langle v^2\rangle + 0.05\,\Delta SB - 0.02(\Delta SB)^2 + 0.69 \log \beta - 1.5\,\delta Mg_2 + 0.85 \log q(M). \quad (8)$$

where $\Delta SB = SB_{\rm e} - SB_n = SB_{\rm e} - 20.75$.

6 CONCLUDING REMARKS

Several questions remain unresolved at this point, in particular how best to estimate the mass from a given set of data, and how to correct luminosities in a given waveband for population differences. An additional problem that must still be considered is that of the *accuracy* and *bias* of the mass–luminosity distance estimator. The inclusion of several, sometimes not precisely measured, quantities in a distance estimator may lead to distances less accurate than those obtained from an approximate expression involving only quantities measured with high precision (such as the D_n–σ relation). On the other hand, the simpler distance estimators (FP and D_n–σ) may be considerably biased in certain regions of parameter space. Ultimately, a simultaneous solution of the mass–luminosity distance indicator and the velocity field is required.

REFERENCES

Bailey M. E., MacDonald J., 1981, MNRAS, 194, 195

Bender R., Burstein D., Faber S. M., 1992, ApJ, 399, 462 (BBF)

Bertin G. et al., 1994, A&A, 292, 381

Binney J., Tremaine S., 1987, Galactic Dynamics. Princeton Univ. Press, Princeton

Binney J. J., Davies R. L., Illingworth G. D., 1990, ApJ, 361, 78 (BDI)

Burstein D., Davies R. L., Dressler A., Faber S. M., Lynden-Bell D., Terlevich R. J., Wegner G., 1988, in Kron R. G., Renzini A., eds, Towards Understanding Galaxies at Large Redshifts. Kluwer, Dordrecht, p. 17

Burstein D., Faber S. M., Dressler A., 1990, ApJ, 354, 18

Carollo C. M., 1993, PhD thesis, Ludwig-Maximilians University, Munich

Carollo C. M., Danziger I. J., 1994, MNRAS, 270, 743

Chandrasekhar S., 1969, Ellipsoidal Figures of Equilibrium. Yale Univ. Press, New Haven

de Carvalho R. R., Djorgovski S., 1992, ApJ, 389, L49

de Vaucouleurs G., de Vaucouleurs A., Corwin H. G., Jr, Buta R. J., Paturel G., Fouqué P., 1991, Third Reference Catalogue of Bright Galaxies. Springer-Verlag, New York (RC3)

Djorgovski S., Davis M., 1987, ApJ, 313, 59

Djorgovski S., Santiago B. X., 1993, in Danziger I. J., Zeilinger W. W., Kjär K., eds, ESO Proc. 45, Structure, Dynamics and Chemical Evolution of Elliptical Galaxies. ESO, Garching, p. 59

Dressler A., 1987, ApJ, 317, 1

Dressler A., Lynden-Bell D., Burstein D., Davies R. L., Faber S. M., Terlevich R. J., Wegner G., 1987, ApJ, 313, 42

Faber S. M., Dressler A., Davies R. L., Burstein D., Lynden-Bell D., Terlevich R. J., Wegner G., 1987, in Faber S. M., ed., Nearly Normal Galaxies, From the Planck Time to the Present. Springer-Verlag, New York, p. 175

Faber S. M., Wegner G., Burstein D., Davies R. L., Dressler A., Lynden-Bell D., Terlevich R. J., 1989, ApJS, 69, 763

Guzmán R., Lucey J. R., 1993, MNRAS, 263, L47

Guzmán R., Lucey J. R., Carter D., Terlevich R. J., 1992, MNRAS, 257, 187

Guzmán R., Lucey J. R., Bower R. G., 1993, MNRAS, 265, 731

Jørgensen I., Franx M., Kjærgaard P., 1993, ApJ, 411, 34 (JFK)

Kraan-Korteweg R. C., 1986, A&AS, 66, 255

Lynden-Bell D., Faber S. M., Burstein D., Davies R. L., Dressler A., Terlevich R. J., Wegner G., 1988, ApJ, 326, 19
Michard R., 1980, A&A, 91, 122
Renzini A., Ciotti L., 1993, ApJ, 416, L49
Saglia R. P., Bender R., Dressler A., 1993, A&A, 279, 75 (SBD)
Satoh C., 1980, PASJ, 32, 41
van Albada T. S., Bertin G., Stiavelli M., 1993, MNRAS, 265, 627
van der Marel R. P., Franx M., 1993, ApJ, 407, 525
Worthey G., 1994, ApJS, 95, 107

APPENDIX A: MODELS OF OBLATE STELLAR SYSTEMS

We have constructed one-component (constant mass-to-light ratio) models of oblate systems with the following procedure. Adopt cylindrical coordinates R, z, ϕ and choose a density profile $\rho(R, z)$. For a distribution function depending on only two integrals of motion, $f=f(E, J_z)$, one may calculate the velocity dispersions by solving Poisson's and Jeans's equations (Satoh 1980; BDI). For ρ we choose a modified Jaffe law:

$$\rho(m)=\rho_0 \frac{1}{(1+m/r_c)^2(1+m/r_L)^2}, \tag{A1}$$

where

$$m^2=R^2+z^2/(c/a)^2. \tag{A2}$$

r_c is the core radius, r_L is the half-mass radius of the unmodified Jaffe law, and c/a is the axis ratio of the system. We use $r_c=0.001 r_L$.

The models yield the dependence of the mean square velocities $\langle v_R^2\rangle$, $\langle v_z^2\rangle$, and $\langle v_\phi^2\rangle$ on R and z. Because there is no streaming in the R and z directions, we write σ_R^2 and σ_z^2 for $\langle v_R^2\rangle$ and $\langle v_z^2\rangle$ respectively. Due to our choice of f, $\sigma_R=\sigma_z$ everywhere. Models of this type leave the odd moments of the velocity distribution undetermined, but streaming in the azimuthal direction can be introduced in an ad hoc manner by defining

$$\langle v_\phi\rangle \equiv k\sqrt{\langle v_\phi^2\rangle - \sigma_R^2}, \tag{A3}$$

where k varies from 0 to 1 (Satoh 1980; BDI). For $k=1$, the model is an 'isotropic rotator', because in that case $\sigma_\phi=\sigma_R=\sigma_z$. For $k=0$, there is no streaming and flattened models have anisotropic pressure.

The models have been projected on the sky for a range of viewing angles, and the mean square velocity $\langle v^2\rangle$ (including rotation if present) has been calculated for circular apertures centred on the galaxy. $R^{1/4}$-laws have been fitted to the major-axis luminosity profiles of the projected images, yielding $R_{e,ma}$. As geometry requires, we find that $R_{e,ma}$ is independent of inclination, to within 0.5 per cent; in the following, we shall therefore use the face-on value R_{e0}. The effective radii R_{ei} of the systems at a viewing angle i are taken as:

$$R_e \equiv \sqrt{R_{e,mi} R_{e,ma}} = R_{e0}\sqrt{p}, \tag{A4}$$

where p is the axis ratio of the isophotes of the projected image. For a density distribution stratified on self-similar ellipsoids, as in equation (A1), p is related to the intrinsic axis ratio c/a and to the inclination i through $p^2=(c/a)^2 \sin^2 i+\cos^2 i$. The code that we use is nearly identical to that of Carollo (1993) and Carollo & Danziger (1994).

It is of interest to compare the model results with predictions from the second-order virial theorem (see Chandrasekhar 1969). Consider a coordinate system x, y, z and let the z-axis coincide with the symmetry axis of our oblate galaxy. Then one may write, using the virial equations in the notation of Binney & Tremaine (1987, section 4.3),

$$K_{xx}/K_{zz}=W_{xx}/W_{zz}. \tag{A5}$$

Here K_{xx} and K_{zz} represent the total kinetic energy in the x and z directions, respectively. (Note that we make no attempt to separate streaming motions from random motions.) The quantities W_{xx} and W_{zz} are diagonal elements of the potential energy tensor. Their ratio depends only on the intrinsic flattening e:

$$\frac{W_{xx}}{W_{zz}}=\frac{1}{2(1-e^2)}\,\frac{\dfrac{\arcsin e}{e}-\sqrt{1-e^2}}{\dfrac{1}{\sqrt{1-e^2}}-\dfrac{\arcsin e}{e}} \equiv G(e), \tag{A6}$$

where $e=\sqrt{1-c^2/a^2}$.

Consider a line of sight x'. From the observational point of view, $K_{x'x'}$ is directly proportional to the luminosity-weighted average over the entire galaxy of the second moment of the velocity profile along x', provided that light traces mass. Then the proportionality factor is simply $0.5M$. For example, for the face-on view x' coincides with the z direction, so that

$$K_{zz} \propto \langle v^2\rangle_0 = \left\langle \int I(x,y,v)(v-v_{sys})^2\,dv \Big/ \int I(x,y,v)\,dv \right\rangle_{x,y}, \tag{A7}$$

where the angular brackets indicate an average over the sky and v_{sys} is the systemic velocity of the object along the line of sight. Thus equation (A5) can be written in the form

$$\langle v^2\rangle_1/\langle v^2\rangle_0=G(e), \tag{A8}$$

where the subscripts 0 and 1 refer to face-on and edge-on view of the system. For an oblate system seen at an inclination i,

$$\langle v^2\rangle_i=\langle v^2\rangle_1 \sin^2 i+\langle v^2\rangle_0 \cos^2 i. \tag{A9}$$

Alternatively, using equation (A8),

$$\langle v^2\rangle_i=\langle v^2\rangle_0[G(e)\sin^2 i+\cos^2 i]. \tag{A10}$$

It should be noted that by taking the second moment of the velocity profile there is only one virial-theorem prediction for the behaviour of $\langle v^2\rangle_i$ with inclination i; the distinction between rotating systems and pressure supported systems is not present.

In Fig. 1, the VT prediction, scaled to our face-on E5 model, is given by the thick solid line. It differs considerably from our model results for an aperture with a radius of $0.5R_e$. Indeed, according to the VT, the quantity $\langle v^2\rangle_i R_{ei}$ is not constant, but varies according to the expression

$$\langle v^2\rangle_i R_{ei}=\langle v^2\rangle_0 R_{e0}[G(e)\sin^2 i+\cos^2 i] \times[(1-e^2)\sin^2 i+\cos^2 i]^{1/4}, \tag{A11}$$

where we have combined equations (A4) and (A10). We have verified that both the pressure-supported models and the oblate isotropic rotators approach the VT prediction when the aperture is increased. For an aperture with a radius of $4R_e$, the difference is less than 2 per cent. Comparing our VT prediction with that using the equations given by SBD, which are based on an approximate analysis (separately for rotating systems and pressure-supported systems), we find significant differences.

APPENDIX B: METALLICITY DEPENDENCE OF THE *L/M* RATIO

Evidence for a spread in L/M at fixed mass, related to the Mg_2 index, is present in the field galaxy sample of Faber et al. (1989). This is shown in Fig. B1. The upper panel displays the $M-Mg_2$ relation, using equation (2) with $\beta = 5$ as the mass estimator. The solid line is a fit with a second-degree polynomial (see caption), and we use this fit to define the metallicity excess at fixed mass as $\delta Mg_2 = (Mg_2)_{\rm obs} - (Mg_2)_{\rm fit}$. In the lower panel of Fig. B1, L_B is plotted against M. Different symbols are used to indicate the values of δMg_2. The data show that, at fixed M, *high* values of L are associated with *lower* than average values of the Mg_2 index. This trend is consistent with the prediction from Worthey's (1994) models.

Plotting the residuals $\delta \log L_B$ with respect to the fitted line versus δMg_2, and applying a χ^2 test to the contingency table based on this plot, we find that the hypothesis that $\delta \log L_B$ and δMg_2 are unrelated can be rejected at the 99 per cent level.

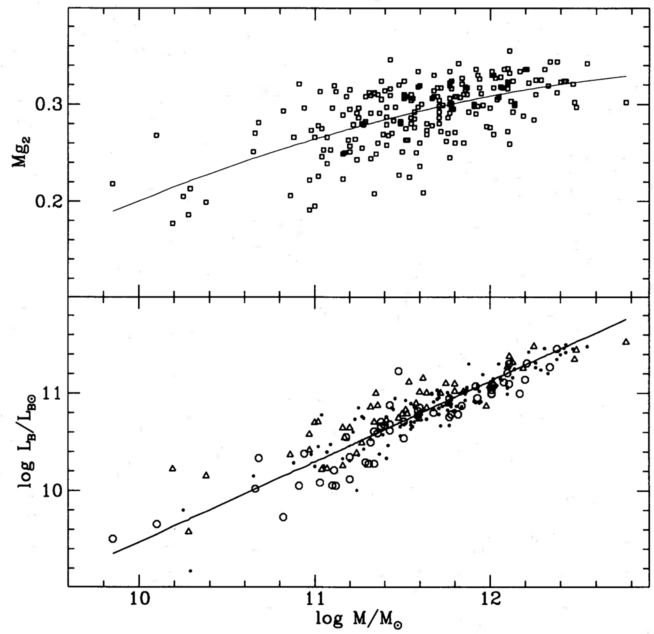

Figure B1. Upper panel: Mg_2 versus M for a sample of 222 field galaxies from Faber et al. (1989). The solid line is the least-squares fit given by: $Mg_2 = 0.20 + 0.073\ (\log M - 10) - 0.010\ (\log M - 10)^2$. It is used to define the metallicity excess $\delta Mg_2 = (Mg_2)_{\rm obs} - (Mg_2)_{\rm fit}$. Lower panel: L_B versus M for the same galaxies as shown in the upper panel. The straight line is a least-squares fit with slope 0.825. Circles: $\delta Mg_2 < -0.02$, triangles: $\delta Mg_2 > 0.02$, small dots: $-0.02 < \delta Mg_2 < 0.02$. Note that the triangles lie mainly above the line, and the circles below. This split according to δMg_2 value shows that luminosity at fixed mass is sensitive to the metallicity excess.